energy&fuels

Article

pubs.acs.org/EF

Changes of Diameter Distribution with Temperature Measured for Asphaltenes and Their Fractions A1 and A2. Impact of These Measurements in Colloidal and Solubility Issues of Asphaltenes

Sócrates Acevedo* and Luis Alejandro García

Universidad Central de Venezuela, Facultad de Ciencias, Escuela de Química, 40756 Caracas, 1053 Venezuela

Pedro Rodríguez

Universidad Central de Venezuela, Facultad de Ciencias, Centro de Microscopía Electrónica 40756 Caracas, 1053 Venezuela

ABSTRACT: Asphaltenes and their fractions A1 (lower solubility) and A2 (higher solubility) were dissolved (3%) in resins and studied at three temperatures (T = 150, 200, and 250 °C), using the combined TEM FF (transmission electron microscopy freeze fracture) technique. In this study, resins coprecipitated with asphaltenes during separation from crude oil were used as solvents. In all solutions, asphaltene particles or nanoaggregates were observed in the range from about 2 to about 12 nm. While for the A2 sample, all calculated average diameters (d_n, d_w, d_z) decrease with temperature, for asphaltenes and A1, the $d_z(T)$ curve have a minimum. For A1 such a minimum was also observed for d_w. These results are coherent with the view in which asphaltene colloids are porous bodies or fractals constituted by molecules of different structure and solubility. Most soluble molecules (A2TM) and molecular aggregates (A2 and A1-A2 type) would prevail both in solution and at the porous colloidal periphery at any T. Solvent held at the periphery would hinder flocculation. When T is raised, a fraction of molecules at the asphaltene colloidal periphery dissolves, thus reducing d_z; however, further increase in T thins the solvent layer, promoting flocculation and thus increasing d_z. Such flocculation is mainly promoted by A1TM. These results, as well as others previously reported, underline the importance of considering asphaltenes as a mixture of compounds with very significant solubility differences, such as the one determined for A1 and A2 fractions. For the temperatures examined, using TEM FF particle density for A1 sample was the highest, which is consistent with its low solubility when compared to asphaltenes and A2.

INTRODUCTION

As suggested by research in the past few years, asphaltenes are a complex mixture of thousands of compounds with molecular mass distribution covering approximately the 200–1000 g mol^{-1} range.[1,2] Though many "impurities" from crude oils, such as paraffin, trapped resins, metal porphyrins, natural surfactants among others have been found in asphaltenes,[3−6] mainly, they are a mixture of similar polycyclic compounds containing condensed aromatic rings and aliphatic rings, aliphatic chains, and heteroatoms (S, N, O). The many components in the mixture, as well as the molecular structure and molecular mass of their components, are expected to determine their colloidal and solubility properties. To illustrate the point of present arguments, we recall that asphaltene colloids or aggregates have been considered as fractals bodies,[7] which, among other considerations, means that they are not capable of covering all the volume they are immersed in.[8] In other words, when the body (aggregate, colloid, or particle) is formed within a media, voids are produced that are immediately filled with media components. This is consistent with trapped compounds isolated from asphaltenes[3] and with the presence of large amounts of coprecipitated resins during common asphaltene isolation from crude oils,[9] which resist complete removal.[10]

Using conductivity measurements, performed with toluene solutions of asphaltenes doped with 0.1 M aqueous HCL, a packing model for asphaltenes was proposed by Sheu.[11] With the HCL probe, linear conductivity−concentration plots were reported, which were coherent with nanoaggregate structures where asphaltenes molecules pack after interlocking each other, leaving holes where solvent is entrapped. In our view, asphaltene fractal colloid structure is the result of aggregate formation by similar but different molecules; by being similar, polar, and of low solubility (A1TM, see below), they promote aggregation, and by being soluble and with differences in structure (A2TM, see below), they promote fractal packing, solvation, and colloidal dispersion.

As reported earlier, asphaltenes contain fractions A1 and A2, where the first have a higher solubility parameter than the second. More than 50 solvents were tested to obtain these solubility parameters, and in all of them, solubility of A2 (measured by the RED parameter) was higher than solubility for A1.[12] In particular, whereas in toluene A2 have a solubility similar to asphaltenes, solubility of A1 is negligible in this solvent. This means that, in toluene solutions of asphaltenes, A1 is solubilized by A2. This argument was found consistent with a multistage aggregation model where low solubility A1 type molecules (A1TM) form aggregates at very low concentrations (around 100 mg L^{-1}) followed by incorporation of A2TM to these aggregates.[13] These arguments are coherent with a model where asphaltenes colloids could be represented

Received: December 12, 2011
Revised: February 13, 2012
Published: February 17, 2012

dx.doi.org/10.1021/ef201947h | *Energy Fuels* 2012, 26, 1814–1819

by means of particles with a core rich in A1-type molecules (A1TM) and a periphery rich in solvent media and A2-type molecules (A2TM). Loose or fractal packing, mainly promoted by A2TM, allows for abundant penetration of solvent at the colloidal periphery, and this solvent held at the periphery would act as a barrier opposing flocculation. Some preliminary features of this model have been described elsewhere.[12]

Besides the above difference in solubility and derived notions about colloidal structure, consideration of asphaltenes as a mixture of A1 and A2 fractions has been found very useful to account for other phenomena such as trapping of compounds (liberated after separation of A1 and A2 fractions[3]), flocculation,[12] aggregation promoted by A1,[14] asphaltene aggregation at very low concentration,[13] and metal distribution.[15] As described below, changes in particle diameter with temperature, measured with the transmission electron microscopy freeze fracture (TEM FF) technique could be accounted for in terms of the above A1-A2 fractal-type model.

EXPERIMENTAL SECTION

Materials. Extra-heavy crude oil, from Hamaca region in Venezuela, with API gravity = 9 and asphaltene content close to 14% was used. Asphaltenes were obtained after heptane addition (40 v) using a modified ASTM procedure.[16] The oil was warmed until it was easily agitated by a mechanical stirrer before heptane addition. The precipitated asphaltene−resins mixture was filtered, washed with hot heptane and transferred to a Soxhlet where resins were extracted with boiling heptane until the emerging heptane became clear (about 5 days). After this, asphaltenes were dried and weighed; the resin-heptane solution was evaporated in a rotatory evaporator under vacuum to obtain the oil resins.

Sample (asphaltenes or A1 or A2)−resins mixtures were prepared by dissolving 800 mg of sample (3% resins) in 50 mL of chloroform. The solutions were refluxed for 3 h, and corresponding sample−resins mixtures were obtained after removal of chloroform, first with a rotatory evaporator and then under vacuum at 60 °C. Complete removal of chloroform was checked with ^{1}H NMR using dichloromethane as solvent.

The reported *p*-nitrophenol procedure was employed for fractionation of asphaltenes in fractions A1 and A2.[17] About 92% of sample was recovered with 59% A1 and 41% A2.

Methods. Thermal treatment of samples was carried out in an steel closed reactor under nitrogen atmosphere. Between 100 and 200 mg of sample−resins mixture was placed in vials within the reactor, along with a bronze holder; after closing it, the mixture was heated at the predetermined temperature during a period of 6 h. After this time, the reactor, kept at the same temperature, was opened, and a tiny amount of sample was transferred to the bronze holder, quickly frozen with under cooled liquid nitrogen, and keep frozen until ready for freeze fracture treatment and MET analysis.

Freeze fracture replicas were obtained using the JEOL JFD 9010C apparatus and the procedure described elsewhere.[18,19] Briefly, frozen samples were placed within the apparatus chamber by clipping the bronze holder in place; the chamber, kept at temperature by a liquid nitrogen jacket, was evacuated at $<10^{-5}$, where it was fractured with the an steel blade kept at −200 °C. This was followed by shadowing, then by evaporation of Pt/C atoms irradiated at 45° (to produce metallic contrast and metallic surface), and after that by C atoms bombarded at 90° (to avoid subsequent ruptures). The sample was then removed and immersed in THF to dissolve all organic material; the replica was then removed with a bronze grid, washed with THF, air-dried, and analyzed with the TEM.

A JEOL, JEM 1220, transmission electron microscopy (TEM) instrument was utilized to view and photograph the sample replicas.[18,19] Photos were taken at 50000× augment, using Kodak film 4489 and copied onto conventional photograph paper at a final augmentation of 100000×. These photos were digitized, and the diameter was measured by densitometry using the Image Tool program with a procedure similar to the one described earlier.[18,19] Briefly, digitizing in .bmp format is followed by calibration of the image; the particle is then selected, and a straight line passing through the particle is drawn; this generates a contrast profile where particle diameter can be measured; the procedure is illustrated in Figure 1.

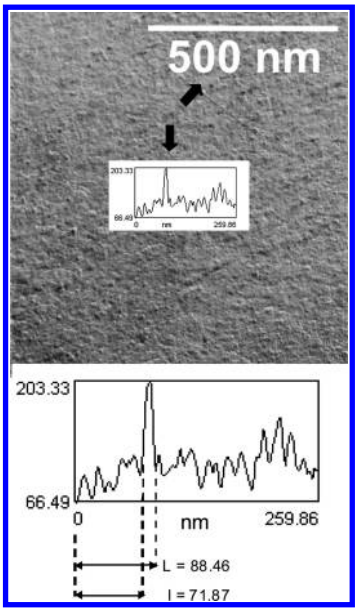

Figure 1. Electron photomicrograph showing how a particle size is measured over a freeze-fracture replica. On the image, arrows are pointing at both the particle and the contrast profile; a calibration bar equal to 500 nm is clearly shown.

These microphotographs show homogeneous colloidal solutions in which insoluble solids were not observed.

RESULTS

All asphaltene−resins mixtures resulted in homogeneous solutions where no insoluble solids could be detected (see the Experimental Section). Figure 2 shows an example of the microphotographs used for both diameter and density calculations.

On the basis of solubility parameters, all samples examined here are expected to be soluble in resins.[12] With the present method, uncertainty in diameter measurement was estimated to be better than ±0.2 nm.

Table 1 shows some statistical results obtained in this work; as usual, these are equivalent diameters, which in our case corresponds to the largest length of the particle being measured. As shown, a large number of particles were measured in an effort to find representative values for samples; mean values and standard deviations were found similar to others reported elsewhere for crude oils using FFMET[18,19] and SAXS[20] measured at comparable temperatures. Standard deviations are large because a wide range of size is being measured.

Table 2 shows results for three mean diameter measured in this work; number (d_n), weight (d_w), and *z*-average (d_z) radius are usual averages defined by eqs 1 to 3; polydispersity p is defined by eq 4.

$$d_n = \frac{\sum_i^n n_i d_i}{\sum_i^n n_i} \quad (1)$$

dx.doi.org/10.1021/ef201947h | Energy Fuels 2012, 26, 1814−1819

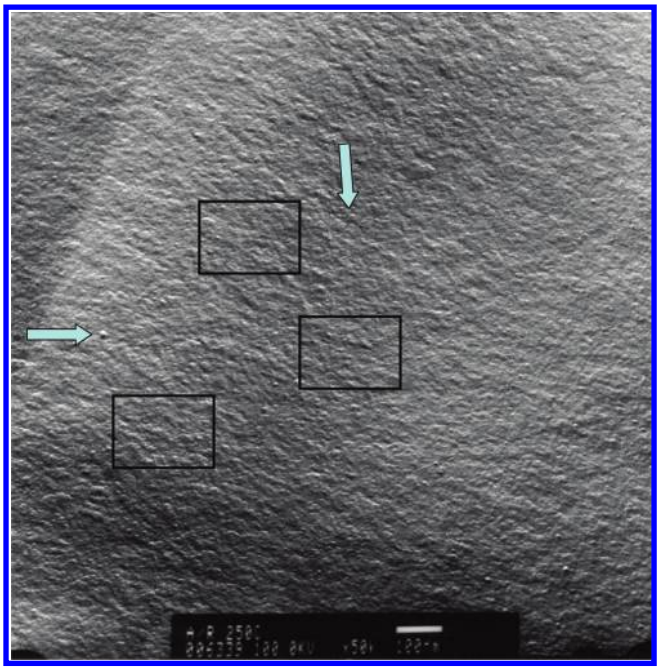

Figure 2. Microphotography corresponding to the asphaltene−resins mixture heated at 250 °C and taken at an augmentation of 100000×. Arrows points to selected particles that look like spheroids. Each particle has a bright and a shadow zone, where the bright zone is the one exposed to metal irradiation at 45°. Square surfaces of 100 nm^2, chosen at random, were used for density measurements. In these, and all over the surface, aggregates of different dimensions and forms could be seen. The white calibration bar, equal to 100 nm, is shown in the inset at the bottom right of the photo.

Table 1. Statistical of Samples Analyzed at Different Temperatures[a]

sample T	n[b]	d_n (mean)[c]	SD[d]	min.[e]	max.[f]
Asp[g] 150	119	6.3	1.4	3.2	10.6
A1 150	163	6.7	1.7	3.3	12.2
A2 150	136	5.6	1.6	3.1	12.4
Asp 200	91	6.2	1.8	3.2	10.4
A1 200	91	6.2	1.8	3.2	10.4
A2 200	109	6.0	1.6	3.1	9.5
Asp 250	107	5.1	2.7	2.2	12.0
A1 250	119	5.1	3.0	2.1	11.3
A2 250	146	3.9	1.3	2.1	6.7

[a]Diameters in nm and temperature in degrees centigrade. [b]Number of particles measured. [c]Ordinary average, equal to d_n. [d]Standard deviation. [e]Minimum diameter. [f]Maximum diameter. [g]Asp: asphaltenes.

$$d_w = \frac{\sum_i^n n_i d_i^2}{\sum_i^n n_i d_i} \tag{2}$$

$$d_z = \frac{\sum_i^n n_i d^3}{\sum_i^n n_i d^2} \tag{3}$$

$$p = \frac{d_w}{d_n} \tag{4}$$

Table 2. Polydispersity p and Number, Weight, and z-Average Particle Diameter Measured at Three Temperatures[a]

sample	d_n[b]	d_w	d_z	p
		150 °C		
Asp	6.3	6.9	7.3	1.10
A1	6.7	7.1	7.5	1.06
A2	5.6	6.0	6.5	1.07
		200 °C		
Asp	6.2	6.8	7.3	1.1
A1	6.2	6.5	6.9	1.07
A2	5.0	5.4	5.8	1.08
		250 °C		
Asp	5.1	6.4	7.9	1.25
A1	5.1	7.0	8.4	1.37
A2	3.9	4.4	4.8	1.13

[a]All diameters in nm. [b]Identical to the mean in Table 1, included here for comparison.

These diameters are special cases of Sauter equivalent diameters given by the general eq 5.

$$d_{pq} = \left(\frac{\sum_i n_i d^p}{\sum_i n_i d^q}\right)^{1/(p-q)} \tag{5}$$

In our case, we have the following: d_n, $p = 1$, $q = 0$; d_w, $p = 2$, $q = 1$; and d_z, $p = 3$, $q = 2$. These diameters are equivalent to averages of sphere dimensions; for instance, diameter d_n is equivalent to length average; d_w is equivalent to area−length average; and d_z is equivalent to volume−area average. Application of these diameters can be found in the literature.[27] Because eqs 1−3 have the same form as the ones corresponding to number, weight, and z molecular mass, we use the same sub index for them; for the same reason, we use eq 4 to define polydispersity.

As expected, the usual trend $d_z > d_w > d_n$ was observed and $p > 1$ in all cases; as one moves from number average to z-average, the averages increases because it becomes more sensitive to changes in the higher diameters. Standard deviations for d_w and d_z were found to be similar to those shown in Table 1 for d_n. Diameters d_w and d_z are particularly helpful in skew distributions such of one found for A1 where a sort of bimodal distribution appears at 250 °C (see Figure 4).

Particle densities measured are shown in Table 3; these were averages of three determinations. As shown, these values are

Table 3. Temperature Dependence of Particle Density (ρ)[a]

	particle density			
T, °C	A1	A2	Asp[c]	A1/A2[b]
150	84 ± 13	49 ± 13	39 ± 6	1.7 ± 0.4
200	80 ± 15	45 ± 5	49 ± 7	1.8 ± 0.3
250	76 ± 15	34 ± 11	38 ± 11	2.2 ± 0.5

[a]Number of particles found in an area equal to 10^4 nm^2. [b]Density ratio. [c]Asphaltenes.

weakly dependent on temperature and values for A1 are the highest. In this work, sample concentration used was the same (3%, see the Experimental Section); hence, differences in ρ among A1 and A2 samples is the consequence of important solubility differences (see the Discussion section).

dx.doi.org/10.1021/ef201947h | Energy Fuels 2012, 26, 1814−1819

As reported by Storm et al.[28] and by Eyssautier[29] et al., diameter reduction during heating would lead to a thinning of solvation shell without significant changes in the number of particles. Thus, the above weak temperature dependence of ρ is expected.

Figures 3−5 show the temperature sequence of diameter distribution for the samples examined. As shown by Figures 3 and 4, two main effects take place when temperature is raised: first, in Figure 3, a shift to smaller diameters is evident, and second, in Figure 4, particle distribution split into two sets of diameters. Apparently, Figure 5, corresponding to asphaltenes, is the result of these two effects combined.

When both d_w and d_z in Table 2 are plotted against temperature, as shown in Figure 6, minimum values were found for asphaltene and A1 samples. For convenience, plots were fitted to second grade polynomials to underline the trends. As shown, both in Figure 6 and Table 2, no minimum for any of the diameter averages was found for A2 sample.

DISCUSSION

The observed increase in both d_w and d_z found for A1 is consistent with lower solubility when compared to A2, where all average diameters were found to decrease (see Table 2 and Figure 3); for asphaltenes, the trend is consistent with the combined effect of these fractions. Thus, again, an important property of asphaltenes in general, and asphaltene aggregation in particular, as is the change of aggregate size with temperature, could be accounted for in terms of fractions A1 and A2. Other important phenomena,[12−15] described above, could be accounted for in the same way (see the Introduction). In spite of this, and judging from publications dealing with relevant colloidal issues, the presence of A1 and A2 is not even mentioned in these works.

The results above suggest that thinning of asphaltene particles during early heating stages is mainly due to removal of A2TM and corresponding solvation resins from the particle periphery; on the other hand, growing during later stages is due to flocculation or molecular redistribution promoted by A1TM present in the particle core. At low enough temperatures, solvent media is held at the particle periphery mainly by A2TM, thus avoiding colloidal flocculation. At higher temperatures, such as 250 °C, the periphery thins, enabling particles to reach interparticle distances close enough to allow for flocculation. This proposition would be the combined temperature effects observed for A1 and A2 (see Figures 3 to 5), that is, with the shift to lower size diameter shown in Figures 3 and 6 observed for A2 and with the increase of both d_w and d_z observed for A1.

Because sample concentration used was the same for the samples studied, the ρ values shown in Table 3 are consistent with lower solubility of A1TM; in other words, compared to A1, a very significant amount of material in asphaltenes and A2 is in solution and can not be detected by the present technique. These results are coherent with the reported solubility parameter for these samples.[12] Moreover, they underline the fact that, even at these high temperatures and in a good solvent, substantial aggregation is observed for a subfraction of A2, as revealed by the significant ρ values measured.

FINAL REMARKS

The colloidal model described above, coherent with the observed average diameter changes, is one of many proposed in the literature[21−26] (see ref 21 for a review). This gathers several features that must be considered and included when proposing colloidal models for asphaltenes: first, asphaltene

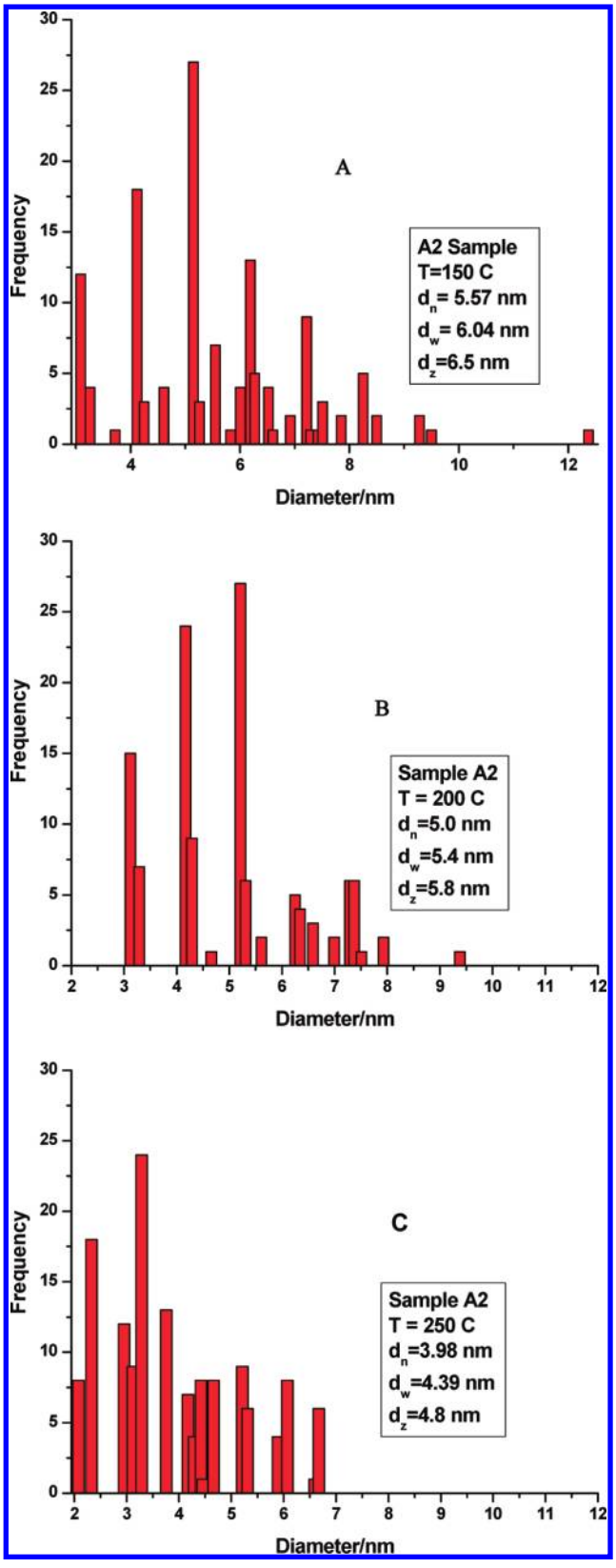

Figure 3. Comparison of diameter distribution for A2 sample: (A) 150 °C; (B) 200 °C; (C) 250 °C. Shift of distribution to smaller diameters is evident and leads to the decrease of all average diameters (see insets and Table 2).

dx.doi.org/10.1021/ef201947h | Energy Fuels 2012, 26, 1814−1819

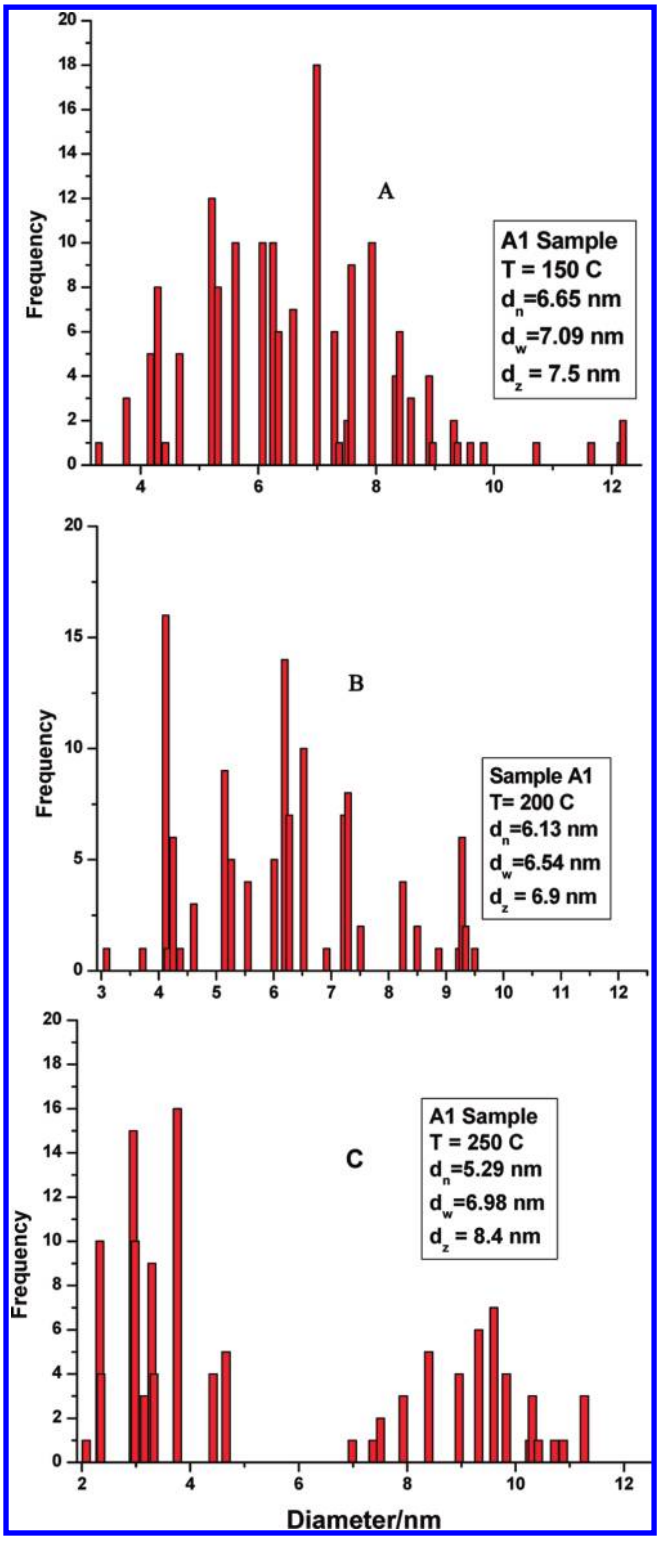

Figure 4. Comparison of diameter distribution for A1 sample: (A) 150 °C; (B) 200 °C; (C) 250 °C. As shown, at 250 °C, the distribution splits into two sets, which leads to increase in d_w, d_z, and p (see insets and Table 2).

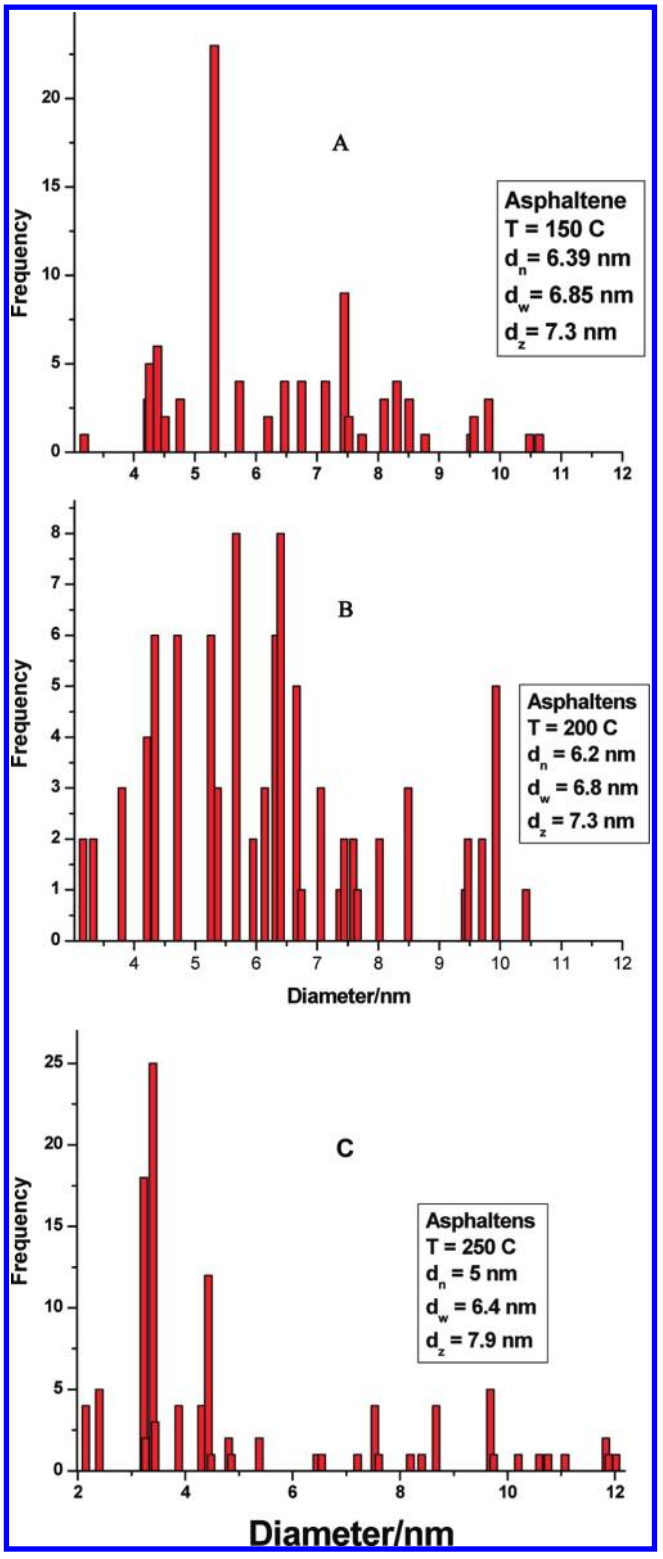

Figure 5. Comparison of diameter distribution for asphaltene sample: (A) 150 °C; (B) 200 °C; (C) 250 °C. Changes in average diameters (decrease in d_w and increase in d_z when changing from 200 to 250 °C) are the combined result of changes for A1 and A2 (see Figures 1 and 2).

molecules cover a wide range of molecular mass and structural types; second, they also cover a wide range of solubility parameters; third, they form loose or fractal aggregates allowing solvent or media to disperse the colloids. Fractal structure is a consequence of aggregation of molecules, similar enough to form aggregates and different enough to lead to lose packing. Low solubility of A1TM promotes aggregation, and high solubility of A2TM promotes dispersion.

As shown elsewhere[12] and corroborated by the density results in Table 3, solubility of asphaltenes follows solubility of A2. This strongly suggest that A1TM are in solution forming

dx.doi.org/10.1021/ef201947h | *Energy Fuels* 2012, 26, 1814–1819

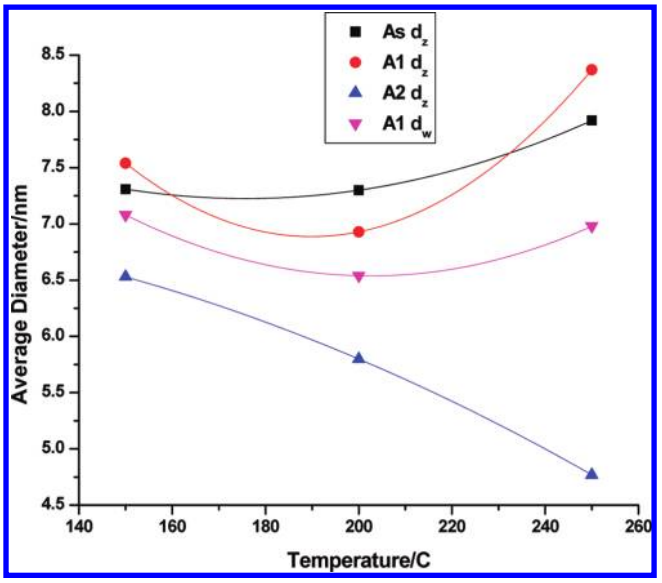

Figure 6. Change of average diameter (d_z or d_w) as function of temperature. To emphasize trends, the points were fitted to second degree polynomial. Note that for A1 both d_w and $d_z$reach minimum values (see also Table 2).

aggregates with A2TM. One could speculate that such aggregates would be similar to intercalation compounds where melting, glass transition, and other solubility related properties are closer to A2TM.

As described above, diameter changes observed are coherent with the general solubility properties of A1 and A2 and, as such, should not depend on asphaltene source. However, it would interesting to perform similar experiments with asphaltenes coming from oils with asphaltene precipitation problems.

AUTHOR INFORMATION

Corresponding Author

*E-mail: socrates.acevedo@ciens.ucv.ve.

Notes

The authors declare no competing financial interest.

ACKNOWLEDGMENTS

The authors acknowledge the CDCH-UCV for providing financing for Project No. CDCH PG 03-5585-2004/I and Lic. Betilde Segovia for administrative assistance.

REFERENCES

(1) Pinkston, D. S.; Duan, P.; Gallardo, V. A.; Habicht, S. C.; Tan, X.; Qian, K.; Gray, M.; Mullen, K.; Kenttamaa., H. I. *Energy Fuels* **2009**, *23*, 5564−5570.

(2) Hortal, A. R.; Hurtado, P.; Martinez-Haya, B.; Mullins, O. C. *Energy Fuels* **2007**, *21* (5), 2863−2868.

(3) Acevedo, S.; Cordero, T.; M, J.; Carrier, H.; Bouyssiere, B.; Lobinsk, R. *Energy Fuels* **2009**, *23*, 842−848.

(4) Liao, Z.; Geng, A.; Graciaa, A.; Creux, P.; Chrostowska, A.; Zhang, Y. *Energy Fuels* **2006**, *20*, 1131−1136.

(5) Liao, Z.; Zhou, H.; Graciaa, A.; Chrostowska, A.; Creux, P.; Geng, A *Energy Fuels* **2005**, *19* (1), 180−186.

(6) Dechaine, G. P.; Gray, M. R. *Energy Fuels* **2010**, *24*, 2795−2808.

(7) Sheu, E. Y. *Asphaltenes: Fundamentals and Applications*; Sheu, E. Y., Mullins, O. C., Eds.; Plenum Press: New York, 1995; Chapter 1.

(8) Vicsek, T. *Fractal Grow Phenomena*; World Scientific Publishing: New Jersey, 1992; Chapter 2.

(9) Acevedo, S.; Layrisse, I.; Méndez, B.; Rivas, H. y; Rojas, A. *Fuel* **1985**, *64* (1741), 1747.

(10) Strausz, O. P.; Torres, M.; Lown, E. M.; Safarik, I.; Murgich, J. *Energy Fuels* **2006**, *20* (5), 2013−2021.

(11) Sheu, E. Y. *Structures and Dynamics of Asphaltenes*; Mullins, O. C., Sheu, E. Y., Eds.; Plenum Press: New York, 1998; Chapter IV, pp 115−144.

(12) Acevedo, S.; Castro, A.; Vasquez, E.; Marcano, F.; Ranaudo, M. A. *Energy Fuels* **2010**, *24*, 5921−5933.

(13) Acevedo, S.; Caetano, M.; Ranaudo, M. A.; Jaimes, B. *Energy Fuels* **2011**, *25*, 3544−3551.

(14) Acevedo, S.; Guzmán, K.; Ocanto, O. *Energy Fuels* **2010**, *24* (3), 1809−1812.

(15) Marcano, F.; Flores, R.; Chirinos, J.; Ranaudo, M. A. *Energy Fuels* **2011**, *25*, 2137−2141.

(16) *Standard test Methods for Determination of Asphaltenes (Heptane Insoluble) in Crude Petroleum and Petroleum Products*, ASTMD 6560; ASTM International: West Conshohocken, PA, 2005.

(17) Gutiérrez, L. B.; Ranaudo, M. A.; Méndez, B.; Acevedo, S. *Energy Fuels* **2001**, *15*, 624−628.

(18) Acevedo, S.; Labrador, H; Rodríguez, P. *Energy Fuels* **2004**, *18*, 1757−1763.

(19) Acevedo, S.; Zuloaga, C.; Rodríguez, P. *Energy Fuels* **2008**, *22*, 2332−2340.

(20) Sheu, E. Y.; Acevedo, S. *Energy Fuels* **2001**, *15*, 702−707.

(21) Sirota, E. B. *Energy Fuels* **2005**, *19*, 1290−1296.

(22) Gray, M. R.; Tykwinski, R. R.; Stryker, J. M.; Tan, X. *Energy Fuels* **2011**, *25*, 3125−3134.

(23) Porte, G.; Zhou, H.; Lazzeri, V. *Langmiur* **2003**, *19*, 40−47.

(24) Fenistain, D.; Barré, L.; Broseta, D.; Espinat, D.; Livet, H.; Roux, J.-N.; Scarsella, M. *Langmiur* **1998**, *14*, 1013−1020.

(25) Leontaritis, K. J. Mansoori, G. A. *Society of Petroleum Engineers International Symposium on Oilfield Chemistry*, San Antonio, TX, 1987.

(26) Victorov, A. I.; Firoozabadi, A. *Am. Inst. Chem. Eng. J.* **1996**, *42*, 1753−1764.

(27) Orr, C. In *Encyclopedia of Emulsion Technology*; Becher, P., Ed.; Marcel Dekker: New York, 1983; Vol. *1*, Chapter 6, p 372.

(28) Storm, D., A.; Barresi, R. J.; Sheu, E., Y. *Energy Fuels* **1995**, *9*, 168−176.

(29) Eyssautier, J.; Hénaut, I.; Levitz, P.; Espinat, D.; Barré, L. *Energy Fuels* **2012**, ASAP.